Free vibration analysis of porous functionally graded plates using a novel shape function

Billel Rebai[a], *Tidjani* Messas[b], *Mustapha* Meradjah[c], *Mohammed* Benali Amar[d]

[a] Faculty of Sciences & Technology, Civil Eng Department, University Abbes Laghrour, Khenchela, Algeria,
e-mail: billel.rebai@univ-khenchela.dz, **corresponding author**,
ORCID iD: https://orcid.org/0000-0003-3739-2784

[b] Faculty of Sciences & Technology, Civil Eng Department, University Abbes Laghrour, Khenchela, Algeria,
e-mail: messas_tidjani@univ-khenchela.dz,
ORCID iD: https://orcid.org/0000-0002-0399-3541

[c] Civil Eng Department, Faculty of Technology, University of Sidi Bel Abbes, Algeria +
Joint Research Team "Nano-Biomaterials and Digital Engineering for Pharmaceutical Applications", Thematic Agency for Research in Science and Technology (ATRST), Algeria,
e-mail: meradjahmustapha@gmail.com,
ORCID iD: https://orcid.org/0000-0002-5988-6120

[d] Civil Eng Department, Faculty of Technology,University of Sidi Bel Abbes, Algeria,
e-mail: mohabenali12@gmail.com,
ORCID iD: https://orcid.org/0000-0002-5988-4567

https://doi.org/10.5937/vojtehg74-59377

FIELD: mechanics, materials, mechanical engineering
ARTICLE TYPE: original scientific paper

Abstract:

Introduction/purpose: This study introduces a novel analytical framework to comprehensively investigate the natural vibration characteristics of porous functionally graded (FG) plates. The research aims to combine an innovative shape function methodology with a sophisticated porosity model within an advanced higher-order shear deformation theory (HSDT).

Methods: Material properties follow power-law distributions across the thickness, with voids incorporated via a refined porosity formulation. The governing equations for simply supported plates are solved analytically

ACKNOWLEDGMENT: The authors express their gratitude for the financial support provided by the University Research and Training Projects (PRFU) under the code A01L02UN220120200004, which plays a vital role in supporting doctoral training in higher education institutions in Algeria.

using the Navier technique. A parametric study examines the effects of power-law index, geometric ratios, and porosity distribution.

Results: Results show exceptional agreement with established theories, revealing significant relationships in which both the power-law index and porosity distribution critically influence natural frequencies. New insights are provided into their coupled effects on vibrational behavior.

Conclusion: This work offers fundamental understanding for optimizing porous FG plate design in advanced engineering applications such as aerospace and structural systems, where weight reduction and vibration control are crucial. It delivers practical guidelines for engineering design and material selection.

Key words: functionally graded plates, porosity, natural vibration, shape function, Hamilton's principle, analytical solution.

Introduction

Functionally graded materials (FGMs) have gained significant attention in recent years due to their unique properties that vary gradually through the thickness. Numerous studies have investigated the vibration behavior of FGM plates and shells using different theories and methods. Zhang & Zhou (2008) presented a theoretical analysis of FGM thin plates based on the physical neutral surface, which simplifies the governing equations compared to classical laminated plate theory. Vel & Batra (2004) developed a three-dimensional exact solution for vibrations of FGM rectangular plates, valid for both thick and thin plates with arbitrary material property variations. Several researchers have employed various plate theories to analyze FGM plates. Zenkour (2005) and Messas et al. (2023) used a sinusoidal shear deformation theory to study buckling and free vibration of FGM sandwich plates. Matsunaga (2008) applied a 2-D higher-order deformation theory to analyze natural frequencies and buckling stresses of FGM plates, considering transverse shear and normal deformations.

The inclusion of porosity effects in FGM plates has been a focus of recent studies. Rezaei & Saidi (2015) and Chitour et al. (2024) presented an exact solution for free vibration of thick rectangular porous plates saturated by inviscid fluid. Rebai (2023) investigated the impact of three homogenization models (Reuss, LRVE, Tamura) on the axial and shear stress of sandwich functionally graded plates (Ti-6A1-4V/ZrO2) subjected to linear and nonlinear thermal loads. Gupta & Talha (2018) examined the influence of porosities on flexural and free vibration responses of FGM plates in thermal environments. Various numerical methods have been employed

to analyze FGM structures. Sharma et al. (2022) used polynomial neural networks for stochastic frequency analysis of laminated composite plates with curvilinear fibers. Swain et al. (2020) and Boutrid et al. (2024) applied perturbation techniques and polynomial neural networks for aeroelastic analysis of laminated composite plates with material uncertainty. Degenerated shell elements have been utilized for vibration analysis of plates and shells. Lee & Han (2001) developed a nine-node assumed natural degenerated shell element for free vibration analysis of plates and shells. Tiwari et al. (2019) used 3D degenerated elements to analyze free vibration of delaminated composite plates. The same authors also formulated an 8-noded degenerated shell finite element for modeling and analysis of laminated composite shell structures (Tiwari et al., 2020). Recent studies have focused on advanced theories and methods for analysing FGM plates with porosities. Rezai et al. (2017) investigated natural frequencies of FGM plates with porosities using a simple four-variable plate theory. Zhao et al. (2009) applied the element-free kp-Ritz method for free vibration analysis of FGM plates. Adhikari & Singh (2019) employed a quasi-3D theory to study the dynamic response of FGM plates on elastic foundations. Several researchers have investigated the effects of piezoelectric layers and various porosity distributions on FGM plates. Van Long et al. (2016) developed a new eight-unknown shear deformation theory for bending and free vibration analysis of FGM plates. Choudhary et al. (2023) studied free vibration response of FGM porous metallic plates embedded with piezoelectric layers. Berkia et al. (2023) explored the free vibration behavior of functionally graded (FG) nano-beams using four homogenization schemes. Kurpa & Shmatko (2024) used the Ritz method combined with R-functions theory to analyze vibrations of porous FGM shallow shells with complex platforms. Shmatko et al. (2023) studied nonlinear free vibrations of FGM porous sandwich plates with complex shapes using R-functions theory and variational methods. Cho (2022) employed a 2D natural element method to analyze static bending and free vibration of FG porous plates, considering various porosity distributions. Vasara et al. (2022) used the differential quadrature method to analyze free vibration of FG porous circular and annular plates with different porosity distributions. Recent studies have also explored the effects of reinforcements in FGM plates. Lazar et al. (2023) investigated free vibration analysis of FGM plates reinforced with carbon nanotubes using an exponential distribution law. Huang et al. (2022) pre-

sented a nonlinear vibration analysis of functionally graded porous plates reinforced by graphene platelets on nonlinear elastic foundations.

This study aims to investigate the natural vibration behavior of porous functionally graded (FG) plates through the application of a novel shape function. Utilizing higher-order shear deformation theory (HSDT), the research examines material property variations across the plate thickness using power-law forms. The introduction of a porosity model allows for the analysis of the effects of void content on the plate's mechanical characteristics. The Navier solution technique is employed to obtain analytical solutions for simply supported FG plates. Key parameters, including the power-law index, side-to-thickness ratio, aspect ratio, and porosity, are examined for their influence on the natural frequencies of FG plates. The findings confirm the efficacy of the new shape function in accurately capturing the vibrational behavior of porous FG plates. This comprehensive analysis offers valuable insights for engineers and designers working with these advanced materials, providing a deeper understanding of how various parameters affect the vibrational properties of porous FG plates in practical applications.

Theoretical formulation

Figure 1 illustrates a functionally graded (FG) plate with dimensions h (thickness), a (length), and b (width). This FG plate is composed of a ceramic-metal mixture, where the material properties vary continuously through the thickness. This variation is governed by the volume fractions of the ceramic and metal constituents, leading to a smooth transition in material composition from the top to the bottom surface.

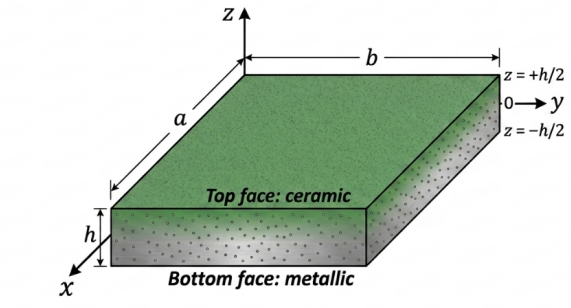

Figure 1 – Geometry of a functionally graded plate

Material property distribution

The homogenization scheme with a power-law distribution is employed to estimate material properties through the thickness. The effective material properties of FG plates are expressed as:

$$P(z) = (P_c - P_m)V_c + P_m \tag{1}$$

where P_c and P_m denote the Young's moduli (E), Poisson's ratios (ν), and mass densities (ρ) of the ceramic and metal materials located at the top and bottom surfaces, respectively. The volume fraction of ceramic material V_c is given by:

$$V_c(z) = \left(\frac{2z+h}{2h}\right)^p \tag{2}$$

where p is the power-law index (positive value) and $z \in [-h/2, h/2]$.

Homogeneous porosity model

Porosity distributions in FG plates can be modeled using various mathematical approaches. This study assumes a homogeneous (even) distribution of porosity throughout the thickness of the FG plate. The presence of porosity reduces the volume fraction of constituent materials as described by:

$$P_{\text{even}} = \frac{\alpha}{2} \tag{3}$$

where α is the porosity coefficient.

Material properties with porosity

The material properties of the porous FG plate vary only in the thickness direction. Using a power-law distribution, the equivalent properties (P) incorporating porosity effects are expressed as:

$$E(z) = (E_c - E_m)V_c(z) + E_m - \frac{\alpha}{2}(E_c + E_m) \tag{4}$$

$$\rho(z) = (\rho_c - \rho_m)V_c(z) + \rho_m - \frac{\alpha}{2}(\rho_c + \rho_m) \tag{5}$$

Limitations of the porosity model

Analysis of Young's modulus and density as functions of porosity coefficient α and material index p reveals critical behavioral thresholds. Minimum values occur when $z \approx -h/2$, p is large, and α is significant. Specifically:

- $E(z) \to 0$ when $\alpha \approx 0.288$ at $z = -h/2$, becoming negative for $\alpha > 0.288$
- $\rho(z) \to 0$ when $\alpha \approx 0.831$ at $z = -h/2$, becoming negative for $\alpha > 0.831$

The findings necessitate limiting α in practical applications to maintain physical validity and structural integrity. The influence of p on property distributions and the significant effect of α on E and ρ values underscore the complex parameter interactions in functionally graded composites.

Kinematics and strains

The displacement field within the higher-order shear deformation theory (HSDT) is expressed as:

$$u(x,y,z) = u_0(x,y) - z\frac{\partial w_0}{\partial x} - f(z)\frac{\partial \phi}{\partial x} \tag{6}$$

$$v(x,y,z) = v_0(x,y) - z\frac{\partial w_0}{\partial y} - f(z)\frac{\partial \phi}{\partial y} \tag{7}$$

$$w(x,y,z) = w_0(x,y) \tag{8}$$

This investigation introduces a novel shape function that satisfies essential continuity conditions and improves analytical accuracy:

$$f(z) = 4.7z\left((z)^{\pi/5} - 0.79\right) \tag{9}$$

The associated strain field is derived from the displacement field as:

$$\boldsymbol{\epsilon} = \boldsymbol{\epsilon}^0 + z\boldsymbol{\kappa}^b + f(z)\boldsymbol{\kappa}^s \tag{10}$$

$$\boldsymbol{\gamma} = g(z)\begin{Bmatrix}\gamma^0_{xz}\\ \gamma^0_{yz}\end{Bmatrix} = g(z)\begin{Bmatrix}\frac{\partial \phi}{\partial x}\\ \frac{\partial \phi}{\partial y}\end{Bmatrix} \tag{11}$$

where $\boldsymbol{\kappa}^b$, $\boldsymbol{\kappa}^s$, and $\boldsymbol{\gamma}^0$ represent bending curvatures, shear curvatures, and transverse shear strains, respectively, with $g(z) = -\frac{df}{dz}$. The strain compo-

nents are defined as:

$$\boldsymbol{\epsilon}^0 = \begin{Bmatrix} \frac{\partial u_0}{\partial x} \\ \frac{\partial v_0}{\partial y} \\ \frac{\partial u_0}{\partial y} + \frac{\partial v_0}{\partial x} \end{Bmatrix} \tag{12}$$

$$\boldsymbol{\kappa}^b = \begin{Bmatrix} -\frac{\partial^2 w_0}{\partial x^2} \\ -\frac{\partial^2 w_0}{\partial y^2} \\ -2\frac{\partial^2 w_0}{\partial x \partial y} \end{Bmatrix} \tag{13}$$

$$\boldsymbol{\kappa}^s = \begin{Bmatrix} -\frac{\partial^2 \phi}{\partial x^2} \\ -\frac{\partial^2 \phi}{\partial y^2} \\ -2\frac{\partial^2 \phi}{\partial x \partial y} \end{Bmatrix} \tag{14}$$

Constitutive relations

The linear constitutive relations for the FG plate are:

$$\begin{Bmatrix} \sigma_{xx} \\ \sigma_{yy} \\ \sigma_{xy} \end{Bmatrix} = \begin{bmatrix} C_{11} & C_{12} & 0 \\ C_{12} & C_{22} & 0 \\ 0 & 0 & C_{66} \end{bmatrix} \begin{Bmatrix} \epsilon_{xx} \\ \epsilon_{yy} \\ \gamma_{xy} \end{Bmatrix} \tag{15}$$

$$\begin{Bmatrix} \sigma_{xz} \\ \sigma_{yz} \end{Bmatrix} = \begin{bmatrix} C_{55} & 0 \\ 0 & C_{44} \end{bmatrix} \begin{Bmatrix} \gamma_{xz} \\ \gamma_{yz} \end{Bmatrix} \tag{16}$$

where the stiffness coefficients are:

$$C_{11}(z) = C_{22}(z) = \frac{E(z)}{1-\nu(z)^2} \tag{17}$$

$$C_{12}(z) = \nu(z) C_{11}(z) \tag{18}$$

$$C_{44}(z) = C_{55}(z) = C_{66}(z) = \frac{E(z)}{2(1+\nu(z))} \tag{19}$$

Equations of motion

Hamilton's principle is employed to derive the equations of motion:

$$\int_0^T (\delta U + \delta K) dt = 0 \tag{20}$$

Rebai, B. et al., Free vibration analysis of porous functionally graded plates using a novel shape function, pp.379–399

where δU and δK represent the variations of strain energy and kinetic energy, respectively. The variation of strain energy is:

$$\delta U = \int_A \begin{bmatrix} N_{xx}\dfrac{\partial \delta u_0}{\partial x} - M^b_{xx}\dfrac{\partial^2 \delta w_0}{\partial x^2} - M^s_{xx}\dfrac{\partial^2 \delta \phi}{\partial x^2} \\ +N_{yy}\dfrac{\partial \delta v_0}{\partial y} - M^b_{yy}\dfrac{\partial^2 \delta w_0}{\partial y^2} - M^s_{yy}\dfrac{\partial^2 \delta \phi}{\partial y^2} \\ +N_{xy}\left(\dfrac{\partial \delta u_0}{\partial y} + \dfrac{\partial \delta v_0}{\partial x}\right) - 2M^b_{xy}\dfrac{\partial^2 \delta w_0}{\partial x \partial y} \end{bmatrix} dA \tag{21}$$

with stress resultants defined as:

$$(N_{xx}, N_{yy}, N_{xy}) = \int_{-h/2}^{h/2} (\sigma_{xx}, \sigma_{yy}, \sigma_{xy}) dz \tag{22}$$

$$(M^b_{xx}, M^b_{yy}, M^b_{xy}) = \int_{-h/2}^{h/2} z(\sigma_{xx}, \sigma_{yy}, \sigma_{xy}) dz \tag{23}$$

$$(M^s_{xx}, M^s_{yy}, M^s_{xy}) = \int_{-h/2}^{h/2} f(z)(\sigma_{xx}, \sigma_{yy}, \sigma_{xy}) dz \tag{24}$$

$$(Q_x, Q_y) = \int_{-h/2}^{h/2} g(z)(\sigma_{xz}, \sigma_{yz}) dz \tag{25}$$

The variation of kinetic energy is given by:

$$\delta K = \int_A \begin{bmatrix} I_0(\dot{u}_0 \delta \dot{u}_0 + \dot{v}_0 \delta \dot{v}_0 + \dot{w}_0 \delta \dot{w}_0) \\ -I_1\left(\dot{u}_0\dfrac{\partial \delta \dot{w}_0}{\partial x} + \dfrac{\partial \dot{w}_0}{\partial x}\delta \dot{u}_0 + \dot{v}_0\dfrac{\partial \delta \dot{w}_0}{\partial y} + \dfrac{\partial \dot{w}_0}{\partial y}\delta \dot{v}_0\right) \\ +I_2\left(\dfrac{\partial \dot{w}_0}{\partial x}\dfrac{\partial \delta \dot{w}_0}{\partial x} + \dfrac{\partial \dot{w}_0}{\partial y}\dfrac{\partial \delta \dot{w}_0}{\partial y}\right) \\ -J_1\left(\dot{u}_0\dfrac{\partial \delta \dot{\phi}}{\partial x} + \dfrac{\partial \dot{\phi}}{\partial x}\delta \dot{u}_0 + \dot{v}_0\dfrac{\partial \delta \dot{\phi}}{\partial y} + \dfrac{\partial \dot{\phi}}{\partial y}\delta \dot{v}_0\right) \\ +K_2\left(\dfrac{\partial \dot{\phi}}{\partial x}\dfrac{\partial \delta \dot{\phi}}{\partial x} + \dfrac{\partial \dot{\phi}}{\partial y}\dfrac{\partial \delta \dot{\phi}}{\partial y}\right) \\ +J_2\left(\dfrac{\partial \dot{w}_0}{\partial x}\dfrac{\partial \delta \dot{\phi}}{\partial x} + \dfrac{\partial \dot{\phi}}{\partial x}\dfrac{\partial \delta \dot{w}_0}{\partial x} + \dfrac{\partial \dot{w}_0}{\partial y}\dfrac{\partial \delta \dot{\phi}}{\partial y} + \dfrac{\partial \dot{\phi}}{\partial y}\dfrac{\partial \delta \dot{w}_0}{\partial y}\right) \end{bmatrix} dA \tag{26}$$

where the inertia terms are:

$$(I_0, I_1, I_2) = \int_{-h/2}^{h/2} (1, z, z^2)\rho(z)dz \tag{27}$$

$$(J_1, J_2, K_2) = \int_{-h/2}^{h/2} (f(z), zf(z), f^2(z))\rho(z)dz \tag{28}$$

Applying integration by parts and collecting coefficients, the equations of motion are obtained:

$$\delta u_0 : \quad \frac{\partial N_{xx}}{\partial x} + \frac{\partial N_{xy}}{\partial y} = I_0\ddot{u}_0 - I_1\frac{\partial \ddot{w}_0}{\partial x} - J_1\frac{\partial \ddot{\phi}}{\partial x} \tag{29}$$

$$\delta v_0 : \quad \frac{\partial N_{xy}}{\partial x} + \frac{\partial N_{yy}}{\partial y} = I_0\ddot{v}_0 - I_1\frac{\partial \ddot{w}_0}{\partial y} - J_1\frac{\partial \ddot{\phi}}{\partial y} \tag{30}$$

$$\begin{aligned}\delta w_0 : \quad & \frac{\partial^2 M^b_{xx}}{\partial x^2} + 2\frac{\partial^2 M^b_{xy}}{\partial x \partial y} + \frac{\partial^2 M^b_{yy}}{\partial y^2} \\ & = I_0\ddot{w}_0 + I_1\left(\frac{\partial \ddot{u}_0}{\partial x} + \frac{\partial \ddot{v}_0}{\partial y}\right) - I_2\nabla^2\ddot{w}_0 - J_2\nabla^2\ddot{\phi}\end{aligned} \tag{31}$$

$$\begin{aligned}\delta \phi : \quad & \frac{\partial^2 M^s_{xx}}{\partial x^2} + 2\frac{\partial^2 M^s_{xy}}{\partial x \partial y} + \frac{\partial^2 M^s_{yy}}{\partial y^2} + \frac{\partial Q_x}{\partial x} + \frac{\partial Q_y}{\partial y} \\ & = J_1\left(\frac{\partial \ddot{u}_0}{\partial x} + \frac{\partial \ddot{v}_0}{\partial y}\right) - J_2\nabla^2\ddot{w}_0 - K_2\nabla^2\ddot{\phi}\end{aligned} \tag{32}$$

where $\nabla^2 = \frac{\partial^2}{\partial x^2} + \frac{\partial^2}{\partial y^2}$ is the Laplacian operator. The stress resultants are expressed in terms of strains as:

$$\begin{Bmatrix} \mathbf{N} \\ \mathbf{M}^b \\ \mathbf{M}^s \end{Bmatrix} = \begin{bmatrix} \mathbf{A} & \mathbf{B} & \mathbf{B}^s \\ \mathbf{B} & \mathbf{D} & \mathbf{D}^s \\ \mathbf{B}^s & \mathbf{D}^s & \mathbf{H}^s \end{bmatrix} \begin{Bmatrix} \boldsymbol{\epsilon}^0 \\ \boldsymbol{\kappa}^b \\ \boldsymbol{\kappa}^s \end{Bmatrix} \tag{33}$$

with stiffness coefficients:

$$(\mathbf{A}, \mathbf{B}, \mathbf{D}, \mathbf{B}^s, \mathbf{D}^s, \mathbf{H}^s) = \int_{-h/2}^{h/2} (1, z, z^2, f(z), zf(z), f^2(z))\mathbf{C}(z)dz \tag{34}$$

The transverse shear forces are:

$$\begin{Bmatrix} Q_x \\ Q_y \end{Bmatrix} = \begin{bmatrix} A^s_{55} & 0 \\ 0 & A^s_{44} \end{bmatrix} \begin{Bmatrix} \gamma^0_{xz} \\ \gamma^0_{yz} \end{Bmatrix} \tag{35}$$

where the shear stiffness components are:

$$A_{44}^s = A_{55}^s = \int_{-h/2}^{h/2} g^2(z) C_{44}(z) dz \tag{36}$$

Analytical solution for simply-supported FG plates

The Navier solution technique is employed to obtain analytical solutions for simply-supported boundary conditions. The displacement functions are expressed as:

$$u_0(x,y,t) = \sum_{m=1}^{\infty}\sum_{n=1}^{\infty} u_{mn}^0 \cos\lambda x \sin\mu y e^{i\omega t} \tag{37}$$

$$v_0(x,y,t) = \sum_{m=1}^{\infty}\sum_{n=1}^{\infty} v_{mn}^0 \sin\lambda x \cos\mu y e^{i\omega t} \tag{38}$$

$$w_0(x,y,t) = \sum_{m=1}^{\infty}\sum_{n=1}^{\infty} w_{mn}^0 \sin\lambda x \sin\mu y e^{i\omega t} \tag{39}$$

$$\phi(x,y,t) = \sum_{m=1}^{\infty}\sum_{n=1}^{\infty} \phi_{mn}^0 \sin\lambda x \sin\mu y e^{i\omega t} \tag{40}$$

where $\lambda = m\pi/a$, $\mu = n\pi/b$, ω is the natural frequency, and $i = \sqrt{-1}$. Substituting these into the equations of motion yields the eigenvalue problem:

$$\left(\begin{bmatrix} k_{11} & k_{12} & k_{13} & k_{14} \\ k_{12} & k_{22} & k_{23} & k_{24} \\ k_{13} & k_{23} & k_{33}+\alpha & k_{34} \\ k_{14} & k_{24} & k_{34} & k_{44} \end{bmatrix} - \omega^2 \begin{bmatrix} m_{11} & 0 & m_{13} & m_{14} \\ 0 & m_{22} & m_{23} & m_{24} \\ m_{13} & m_{23} & m_{33} & m_{34} \\ m_{14} & m_{24} & m_{34} & m_{44} \end{bmatrix} \right) \begin{Bmatrix} u_{mn}^0 \\ v_{mn}^0 \\ w_{mn}^0 \\ \phi_{mn}^0 \end{Bmatrix} = \begin{Bmatrix} 0 \\ 0 \\ 0 \\ 0 \end{Bmatrix} \tag{41}$$

where the stiffness and mass matrix components are defined as:

$$\begin{aligned}
k_{11} &= A_{11}\lambda^2 + A_{66}\mu^2 \\
k_{12} &= (A_{12} + A_{66})\lambda\mu \\
k_{13} &= -B_{11}\lambda^3 - (B_{12} + 2B_{66})\lambda\mu^2 \\
k_{14} &= -B_{11}^s\lambda^3 - (B_{12}^s + 2B_{66}^s)\lambda\mu^2 \\
k_{22} &= A_{66}\lambda^2 + A_{22}\mu^2 \\
k_{23} &= -B_{22}\mu^3 - (B_{12} + 2B_{66})\lambda^2\mu
\end{aligned}$$

$$
\begin{aligned}
k_{24} &= -B^s_{22}\mu^3 - (B^s_{12} + 2B^s_{66})\lambda^2\mu \\
k_{33} &= D_{11}\lambda^4 + 2(D_{12} + 2D_{66})\lambda^2\mu^2 + D_{22}\mu^4 \\
k_{44} &= H^s_{11}\lambda^4 + 2(H^s_{12} + 2H^s_{66})\lambda^2\mu^2 + A^s_{55}\lambda^2 + A^s_{44}\mu^2 + H^s_{22}\mu^4 \\
m_{11} &= m_{22} = I_0 \\
m_{13} &= -\lambda I_1 \\
m_{14} &= -\lambda J_1 \\
m_{23} &= -\mu I_1 \\
m_{24} &= -\mu J_1 \\
m_{33} &= I_0 + I_2(\lambda^2 + \mu^2) \\
m_{34} &= J_2(\lambda^2 + \mu^2) \\
m_{44} &= K_2(\lambda^2 + \mu^2) \\
\alpha &= -N_0(\lambda^2 + \gamma\mu^2)
\end{aligned}
$$

Numerical results and discussion

Comparisons and validation

This study examines a simply supported functionally graded (FG) rectangular plate with dimensions a (length) and b (width). Two material combinations are investigated: Al/Al_2O_3 and Al/ZrO_2, with their properties detailed in Table 1.

Table 1 – Material properties of metal and ceramic constituents

Material	Young's modulus (GPa)	Mass density (kg/m^3)	Poisson's ratio
Aluminum (Al)	70	2,702	0.3
Zirconia (ZrO_2)	151	3,000	0.3
Alumina (Al_2O_3)	380	3,800	0.3

The research presents numerical validation and explores how the power-law index (p) and side-to-thickness ratio (a/h) influence the natural frequencies of FG plates. Non-dimensional frequency parameters are employed throughout:

$$\overline{\omega} = \frac{\omega a^2}{h}\sqrt{\frac{\rho_c}{E_c}} \tag{42}$$

$$\overline{\beta} = \frac{\omega ab}{\pi^2 h}\sqrt{\frac{12(1-\nu_c^2)\rho_c}{E_c}} \tag{43}$$

Tables 2 and 3 present comparative analyses of non-dimensional frequencies for FG square plates. Table 2 focuses on Al/Al_2O_3 plates, while Table 3 examines Al/ZrO_2 plates, both showcasing results for various power-law indices (p) and aspect ratios.

Table 2 – Non-dimensional natural frequencies ($\bar{\omega}$) of Al/Al_2O_3 square plates

l/h	Mode (m,n)	Theory	p					
			0	0.5	1	2	5	10
5	(1,1)	Nguyen (2015)	5.2932	4.5258	4.0860	3.6859	3.3919	3.2574
		Present	5.2817	4.5248	4.0932	3.7023	3.4088	3.9730
	(1,2)	Nguyen (2015)	11.6113	10.0109	9.0538	8.1181	7.2951	6.9568
		Present	11.5590	9.9833	9.0404	8.1226	7.3120	9.8089
	(2,2)	Nguyen (2015)	16.8351	14.5888	13.2140	11.8101	10.4647	9.9360
		Present	16.7275	14.5031	13.1210	11.7231	10.4234	9.8591
10	(1,1)	Nguyen (2015)	5.7731	4.9031	4.4216	4.0105	3.7671	3.6388
		Present	5.7695	4.9209	4.4629	4.0743	3.8198	3.6644
	(1,2)	Nguyen (2015)	13.7855	11.7519	10.6036	9.5884	8.9042	8.5729
		Present	13.7656	11.7807	10.6840	9.7180	9.0138	8.6192
	(2,2)	Nguyen (2015)	21.1728	18.1033	16.3438	14.7435	13.5677	13.0296
		Present	21.1270	18.0995	16.3728	14.8092	13.6354	13.0383
20	(1,1)	Nguyen (2015)	5.9209	5.0176	4.5234	4.1104	3.8880	3.7629
		Present	5.9198	5.0490	4.5923	4.2145	3.9730	3.8075
	(1,2)	Nguyen (2015)	14.6131	12.3983	11.1785	10.1482	9.5645	9.2471
		Present	14.6073	12.4863	11.3767	10.4479	9.8089	9.3740
	(2,2)	Nguyen (2015)	23.0925	19.6126	17.6865	16.0419	15.0685	14.5550
		Present	23.0781	19.6839	17.8519	16.2972	15.2792	14.6576

Table 3 – Comparison of non-dimensional fundamental frequency ($\bar{\beta}$) of Al/ZrO_2 square plates

l/h	Theory	p							
		0	0.1	0.2	0.5	1	2	5	10
5	Present	1.7684	1.7218	1.6827	1.5984	1.5226	1.4617	1.4067	1.3695
	Nguyen (2015)	1.7723	1.7241	1.6850	1.6003	1.5245	1.4629	1.4084	1.3726
	Sekkal (et al.)	1.7723	1.7256	1.6866	1.6040	1.5297	1.4691	1.4121	1.3743
10	Present	1.9317	1.8787	1.8347	1.7420	1.6623	1.6034	1.5522	1.5096
	Nguyen (2015)	1.9330	1.8783	1.8342	1.7402	1.6593	1.5994	1.5500	1.5095
	Sekkal (et al.)	1.9330	1.8799	1.8361	1.7445	1.6657	1.6071	1.5548	1.5116
20	Present	1.9820	1.9270	1.8815	1.7868	1.7069	1.6493	1.5991	1.5542
	Nguyen (2015)	1.9824	1.9257	1.8799	1.7830	1.7006	1.6417	1.5945	1.5524
	Sekkal (et al.)	1.9824	1.9273	1.8819	1.7875	1.7075	1.6500	1.5996	1.5547
50	Present	1.9970	1.9414	1.8957	1.8008	1.7215	1.6646	1.6142	1.5680
	Nguyen (2015)	1.9971	1.9398	1.8935	1.7957	1.7129	1.6544	1.6079	1.5653
	Sekkal (et al.)	1.9971	1.9414	1.8955	1.8002	1.7199	1.6628	1.6131	1.5676
100	Present	1.9992	1.9435	1.8978	1.8032	1.7241	1.6675	1.6168	1.5702
	Nguyen (2015)	1.9993	1.9418	1.8955	1.7975	1.7147	1.6562	1.6098	1.5671
	Sekkal (et al.)	1.9993	1.9434	1.8974	1.8021	1.7216	1.6646	1.6150	1.5694

The results demonstrate excellent agreement with established theories by Nguyen (2015) and Sekkal et al. (2017), validating the accuracy of the

novel shape function approach. This analysis confirms the method's reliability and its ability to capture the effects of geometric ratios and material gradation on FG plate vibration characteristics.

Parametric study

Effect of side-to-thickness ratio (a/h) and porosity (α)

Figure 2 illustrates the significant impact of side-to-thickness ratio (a/h) and porosity (α) on the frequencies of square plates. As a/h increases, both natural ($\overline{\omega}$) and fundamental ($\overline{\beta}$) frequencies rise, with the effect being more pronounced at lower ratios. For instance, as a/h increases from 5 to 100, $\overline{\omega}$ increases from 3.70 to 4.29 for non-porous plates.

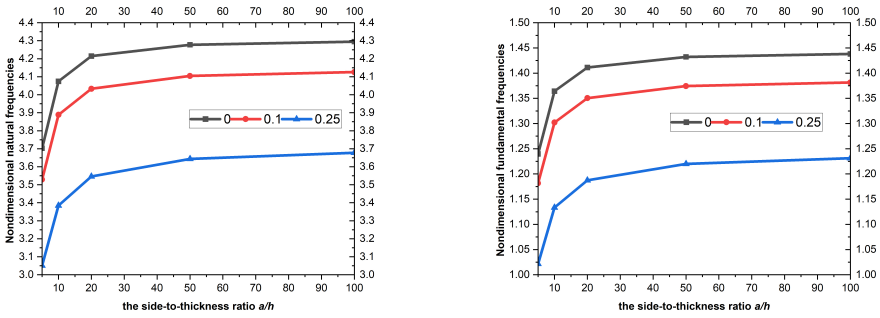

(a) Natural frequency ($\overline{\omega}$) *(b) Fundamental frequency ($\overline{\beta}$)*

Figure 2 – Effect of a/h and α on frequencies of Al/Al$_2$O$_3$ plates ($p = 2$)

Porosity reduces both frequency types consistently across all a/h ratios. At $a/h = 5$, $\overline{\omega}$ decreases from 3.70 to 3.05 as α increases from 0 to 0.25. The combined effect shows that while higher a/h ratios maintain higher frequencies, increased porosity mitigates this effect.

Effect of aspect ratio (a/b) and porosity (α)

Figure 3 demonstrates the influence of aspect ratio (a/b) and porosity on frequencies. As a/b increases, both frequency types rise substantially. When a/b increases from 1 to 10, $\overline{\omega}$ increases from 4.07 to 107.15 for non-porous plates.

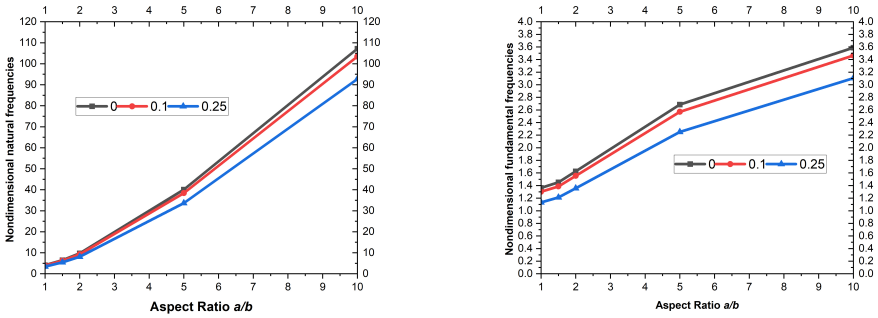

(a) Natural frequency ($\overline{\omega}$) *(b) Fundamental frequency ($\overline{\beta}$)*

Figure 3 – Effect of a/b and α on frequencies of Al/Al$_2$O$_3$ plates ($p = 2$)

Figure 4 provides a three-dimensional visualization of the aspect ratio and porosity effects. The nonlinear increase in $\overline{\omega}$ is particularly evident at higher aspect ratios. Porosity consistently reduces frequencies across all aspect ratios, with $\overline{\omega}$ decreasing from 4.07 to 3.38 at $a/b = 1$ as α increases from 0 to 0.25.

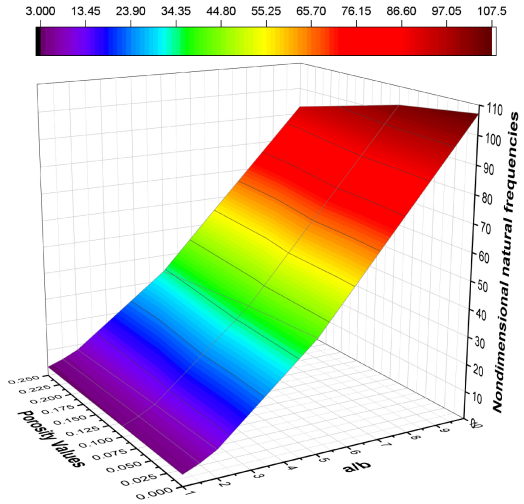

Figure 4 – 3D visualization of the effect of a/b and α on the natural frequency $\overline{\omega}$ for Al/Al$_2$O$_3$ plates ($p = 2$)

Effect of power-law index (p) and porosity (α)

Figure 5 shows the influence of power-law index (p) and porosity on frequencies. As p increases, both frequency types decrease. With $\alpha = 0$, $\overline{\omega}$ decreases from 5.77 at $p = 0$ to 3.22 at $p = 50$.

The rate of decline is most pronounced at lower p values. Porosity consistently reduces frequencies across all p values, with the most significant reductions occurring at higher p values. The combined effect shows a compounded frequency decrease, with the lowest $\overline{\omega} = 2.09$ occurring at $p = 50$ and $\alpha = 0.25$.

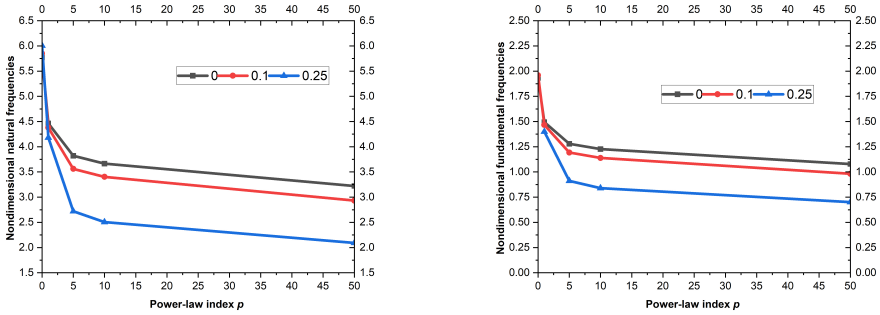

(a) Natural frequency ($\overline{\omega}$) *(b) Fundamental frequency ($\overline{\beta}$)*

Figure 5 – Effect of p and α on frequencies of Al/Al$_2$O$_3$ plates

Effect of mode shapes (m, n) and porosity (α)

Figure 6 illustrates the impact of mode shapes and porosity on natural frequency. As mode numbers increase, $\overline{\omega}$ rises substantially. With $\alpha = 0$, $\overline{\omega}$ increases from 4.46 for (1,1) to 31.50 for (4,1). Porosity reduces $\overline{\omega}$ uniformly across all modes. For mode (2,1), $\overline{\omega}$ decreases from 10.61 at $\alpha = 0$ to 9.89 at $\alpha = 0.25$. The reduction is more significant in absolute terms for higher modes, though the relative reduction remains consistent across modes.

These findings emphasize the need for balanced design approaches that optimize both geometric parameters (a/h, a/b), material composition (p), and porosity (α) to achieve desired vibrational characteristics in engineering applications.

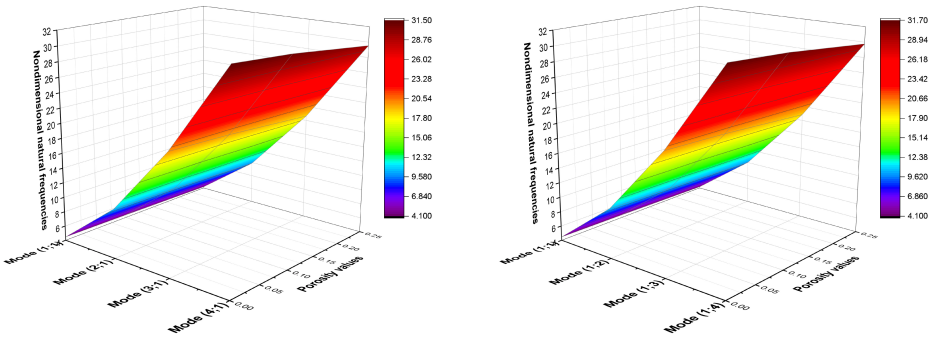

(a) Mode (1,1) to (4,1) *(b) Mode (1,1) to (1,4)*

Figure 6 – Effect of mode shapes and α on $\overline{\omega}$ (Al/Al$_2$O$_3$ plates)

Conclusion

In this study, the natural vibration behavior of porous functionally graded (FG) plates was thoroughly investigated using a novel shape function. A higher-order shear deformation theory (HSDT) was adopted to capture the variation of material properties through the plate thickness using a power-law distribution. Additionally, the inclusion of a porosity model allowed for the assessment of how void content affects the mechanical performance of the plates.

By applying the Navier solution technique, analytical solutions were obtained for simply supported FG plates. A comprehensive parametric study was conducted, considering the effects of power-law index, side-to-thickness ratio, aspect ratio, and porosity on the natural frequencies. The proposed shape function proved effective in precisely modeling the dynamic behavior of porous FG plates.

The results demonstrated that both material gradation and porosity significantly influence the vibrational response of FG structures. These findings provide valuable insights for engineers and researchers in optimizing the design and performance of FG plates in advanced structural applications. The proposed methodology serves as a reliable analytical tool for predicting the dynamic response of such advanced composite systems.

References

Adhikari, B. & Singh, B.N. 2019. Dynamic response of functionally graded plates resting on two-parameter-based elastic foundation model using a quasi-3D theory. *Mechanics Based Design of Structures and Machines*, 47(4), pp.399–429. Available at: https://doi.org/10.1080/15397734.2018.1555965

Berkia, A., Rebai, B., Litouche, B., Abbas, S. & Mansouri, K. 2023. Investigating parametric homogenization models for natural frequency of FGM nano beams. *AIMS Materials Science*, 10(5). Available at: https://doi.org/10.3934/matersci.2023048

Boutrid, A., Rebai, B., Mamen, B., Bouhadra, A. & Tounsi, A. 2024. Combined effect of temperature dependent material properties and boundary conditions on non-linear thermal stability of porous FG beams. *Acta Mechanica*, 235(5), pp.2867–2887. Available at: https://doi.org/10.1007/s00707-024-03860-y

Chitour, M., Khadraoui, F., Mansouri, K., Rebai, B., Menasria, A., Zemmouri, A., ... & Boumediri, H. 2024. A novel high order theory for static bending of functionally graded (FG) beams subjected to various mechanical loads. *Research on Engineering Structures and Materials*, 10. Available at: http://dx.doi.org/10.17515/resm2024.141me0104rs

Choudhary, P.K., Kumar, R. & Kumar, S. 2023. Free Vibration Response of Functionally Graded Porous Metallic Plates Embedded with Piezoelectric Layers. *Journal of Mines, Metals & Fuels*, 71(10). Available at: http://dx.doi.org/10.18311/jmmf/2023/35867

Cho, J.R. 2022. Natural Element Static and Free Vibration Analysis of Functionally Graded Porous Composite Plates. *Applied Sciences*, 12(22), 11648. Available at: https://doi.org/10.3390/app122211648

Gupta, A. & Talha, M. 2018. Influence of porosity on the flexural and free vibration responses of functionally graded plates in thermal environment. *International Journal of Structural Stability and Dynamics*, 18(01), 1850013. Available at: https://doi.org/10.1142/S021945541850013X

Huang, X., Wang, C., Wang, J. & Wei, N. 2022. Nonlinear vibration analysis of functionally graded porous plates reinforced by graphene platelets on nonlinear elastic foundations. *Strojniški vestnik-Journal of Mechanical Engineering*, 68(9), pp.571-582. Available at: https://doi.org/10.5545/sv-jme.2022.274

Kurpa, L. & Shmatko, T. 2024. Research of Vibration Behavior of Porous FGM Panels by the Ritz Method. In *Selected Problems of Solid Mechanics and Solving Methods* (pp. 325-338). Cham: Springer Nature Switzerland. Available at: https://doi.org/10.1007/978-3-031-54063-9_22

Lazar, M.E., Ezzraimi, M., Tiberkak, R., Chiker, Y., Bachene, M. & Rechak, S. 2023. Vibration analysis of composite plates reinforced CNTs using an exponential function approach. *Materials Science and Technology*, 39(17), pp.2680-2689. Available at: https://doi.org/10.1080/02670836.2023.2213975

Lee, S.J. & Han, S.E. 2001. Free-vibration analysis of plates and shells with a nine-node assumed natural degenerated shell element. *Journal of Sound and Vibration*, 241(4), pp.605-633. Available at: https://doi.org/10.1006/jsvi.2000.3313

Matsunaga, H. 2008. Free vibration and stability of functionally graded shallow shells according to a 2D higher-order deformation theory. *Composite structures*, 84(2), pp.132-146. Available at: https://doi.org/10.1016/j.compstruct.2007.07.006

Messas, T., Rebai, B., Mansouri, K., Chitour, M., Berkia, A. & Litouche, B. 2023. Analyzing vibration behavior of Nano FGM (Si_3N_4/SUS304) plates: Impact of homogenization models and nano parameters. *Journal of Nano- and Electronic Physics*, 15(6), 06018. Available at: https://doi.org/10.21272/jnep.15(6).06018

Nguyen, T.K. 2015. A higher-order hyperbolic shear deformation plate model for analysis of functionally graded materials. *International Journal of Mechanics and Materials in Design*, 11(2), pp.203-219. Available at: https://doi.org/10.1007/s10999-014-9260-3

Rebai, B. 2023. Contribution to study the effect of (Reuss, LRVE, Tamura) models on the axial and shear stress of sandwich FGM plate (Ti-6A1-4V/ZrO_2) subjected on linear and nonlinear thermal loads. *AIMS Materials Science*, 10(1). Available at: https://doi.org/10.3934/matersci.2023002

Rebai, B., Mansouri, K., Chitour, M., Berkia, A., Messas, T., Khadraoui, F. & Litouche, B. 2023. Effect of idealization models on deflection of functionally graded material (FGM) plate. *Journal of Nano- and Electronic Physics*, 15(1), 01022. Available at: https://doi.org/10.21272/jnep.15(1).01022

Rezaei, A.S. & Saidi, A.R. 2015. Exact solution for free vibration of thick rectangular plates made of porous materials. *Composite Structures*, 134, pp.1051-1060. Available at: https://doi.org/10.1016/j.compstruct.2015.08.125

Rezaei, A.S., Saidi, A.R., Abrishamdari, M. & Mohammadi, M.P. 2017. Natural frequencies of functionally graded plates with porosities via a simple four variable plate theory: an analytical approach. *Thin-Walled Structures*, 120, pp.366-377. Available at: https://doi.org/10.1016/j.tws.2017.08.003

Sekkal, M., Tounsi, A., Fahsi, B. & Mahmoud, S.R. 2017. A novel and simple higher order shear deformation theory for stability and vibration of functionally graded sandwich plate. *Steel and Composite Structures*, 25(4), pp.389-401. Available at: https://doi.org/10.12989/scs.2017.25.4.389

Sharma, N., Swain, P.K., Maiti, D.K. & Singh, B.N. 2022. Stochastic frequency analysis of laminated composite plate with curvilinear fiber. *Mechanics of Advanced Materials and Structures*, 29(6), pp.933-948. Available at: https://doi.org/10.1080/15376494.2020.1800152

Shmatko, T., Kurpa, L. & Lacarbonara, W. 2023. Nonlinear Free Vibrations of Functionally Graded Porous Sandwich Plates with Complex Shape. In *International Conference on Nonlinear Dynamics and Applications* (pp. 203-215). Cham: Springer Nature Switzerland. Available at: https://doi.org/10.1007/978-3-031-50631-4_18

Swain, P.K., Sharma, N., Maiti, D.K. & Singh, B.N. 2020. Aeroelastic analysis of laminated composite plate with material uncertainty. *Journal of Aerospace Engineering*, 33(1), 04019111. Available at: https://doi.org/10.1061/(ASCE)AS.1943-5525.0001110?

Tiwari, P., Barman, S.K., Maiti, D.K. & Maity, D. 2019. Free vibration analysis of delaminated composite plate using 3D degenerated element. *Journal of Aerospace Engineering*, 32(5), 04019070. Available at: https://doi.org/10.1061/(ASCE)AS.1943-5525.0001053

Tiwari, P., Maiti, D.K. & Maity, D. 2020. Dynamic analysis of composite cylinders using 3-D degenerated shell elements. In *Recent Advances in Theoretical, Applied, Computational and Experimental Mechanics: Proceedings of ICTACEM 2017* (pp. 261-276). Singapore: Springer Singapore. Available at: https://doi.org/10.1007/978-981-15-1189-9_22

Van Long, N., Quoc, T.H. & Tu, T.M. 2016. Bending and free vibration analysis of functionally graded plates using new eight-unknown shear deformation theory by finite-element method. *International journal of advanced structural engineering*, 8(4), pp.391-399. Available at: https://doi.org/10.1007/s40091-016-0140-y

Vasara, D., Khare, S., Sharma, H.K. & Kumar, R. 2022. Free vibration analysis of functionally graded porous circular and annular plates using differential quadrature method. *Forces in Mechanics*, 9, 100126. Available at: https://doi.org/10.1016/j.finmec.2022.100126

Vel, S.S. & Batra, R.C. 2004. Three-dimensional exact solution for the vibration of functionally graded rectangular plates. *Journal of Sound and Vibration*, 272(3-5), pp.703-730. Available at: https://doi.org/10.1016/S0022-460X(03)00412-7

Zhang, D.G. & Zhou, Y.H. 2008. A theoretical analysis of FGM thin plates based on physical neutral surface. *Computational Materials Science*, 44(2), pp.716-720. Available at: https://doi.org/10.1016/j.commatsci.2008.05.016

Zenkour, A.M. 2005. A comprehensive analysis of functionally graded sandwich plates: Part 2—Buckling and free vibration. *International Journal of Solids and Structures*, 42(18-19), pp.5243-5258. Available at: https://doi.org/10.1016/j.ijsolstr.2005.02.016

Zhao, X., Lee, Y.Y. & Liew, K.M. 2009. Free vibration analysis of functionally graded plates using the element-free kp-Ritz method. *Journal of sound and Vibration*, 319(3-5), pp.918-939. Available at: https://doi.org/10.1016/j.jsv.2008.06.025

Analiza slobodnih vibracija poroznih funkcionalno gradiranih ploča primenom nove funkcije oblika

Billel Rebai[a], **autor za prepisku**, *Tidjani* Messas[a], *Mustapha* Meradjah[b], *Mohammed* Benali Amar[c]

[a] Faculty of Sciences & Technology, Civil Eng Department, University Abbes Laghrour, Khenchela, Algeria

[b] Civil Eng Department, Faculty of Technology, University of Sidi Bel Abbes, Algeria +
Joint Research Team “Nano-Biomaterials and Digital Engineering for Pharmaceutical Applications”, Thematic Agency for Research in Science and Technology (ATRST), Algeria

[c] Civil Eng Department, Faculty of Technology, University of Sidi Bel Abbes, Algeria

OBLAST: mehanika, materijali, mašinstvo
KATEGORIJA (TIP) ČLANKA: originalni naučni rad

Sažetak:

Uvod/cilj: Ovo istraživanje uvodi novi analitički okvir za sveobuhvatno ispitivanje prirodnih karakteristika vibracija poroznih funkcionalno gradiranih (FG) ploča. Istraživanje ima za cilj kombinovanje inovativne metodologije funkcije oblika sa naprednim modelom poroznosti u okviru teorije smicajne deformacije višeg reda (eng. HSDT).

Metode: Materijalne karakteristike prate raspodelu po zakonu stepena kroz debljinu, pri čemu su šupljine obuhvaćene unapređenim modelom poroznosti. Diferencijalne jednačine za ploče sa prostim oslanjanjem rešene su analitički primenom Navijeove metode. Parametarskom analizom ispituje se uticaj indeksa zakona stepena, geometrijskih odnosa i raspodele poroznosti.

Rezultati: Rezultati pokazuju izuzetno slaganje sa postojećim teorijama i otkrivaju značajne zavisnosti, pri čemu i indeks zakona stepena i raspodela poroznosti imaju ključan uticaj na sopstvene frekvencije. Dobijeni su novi uvidi u njihove međusobne (spregnute) efekte na vibraciono ponašanje.

Zaključak: Rad omogućava fundamentalno razumevanje optimizacije dizajna poroznih FG ploča u naprednim inženjerskim primenama kao što su vazduhoplovni i konstrukcioni sistemi, gde su smanjenje mase i kontrola vibracija od ključnog značaja. Takođe nudi i praktične smernice za inženjerski dizajn i izbor materijala.

Ključne reči: funkcionalno gradirane ploče, poroznost, sopstvene vibracije, funkcija oblika, Hamiltonov princip, analitičko rešenje.

Paper received on: 8 June 2025.
Manuscript corrections submitted on: 3 October 2025.
Paper accepted for publishing on: 21 November 2025.